University Of Reading
School of Mathematics, Meteorology & Physics

Forward and Inverse Water-Wave Scattering by Topography

by
Christopher R Warner

August 2008

This dissertation is submitted to the Department of Mathematics in partial fulfilment of the requirements for the degree of Master of Science

Abstract

As a plane water-wave passes over a fixed underlying bed topography it scatters and a reflected wave is created travelling in the opposite direction. With knowledge of the incident wave and underlying bed topography, the reflected wave can be calculated; this is known as *forward scattering*.

Taking this reflected data we have formulated the *inverse scattering* problem, whereby we use this data in an iterative process working backwards in an effort to approximate the bed topography. This has been done using both a shallow water, and mild-slope hypothesis.

It is found that the mild-slope approximation is more accurate and reliable than the shallow water approximation at estimating the bed profile. Moreover, it is shown that with a small range of reflected data, $R(\nu)$, and some prior knowledge that the bed profile is mild, the iterative inverse method with the mild-slope approximation is able to produce an accurate representation of the underlying topography.

Acknowledgments

On the administrative side of things I would like to thank EPSRC for their financial support of the Master programme 2007-2008, and Sue Davis for all her help and guidance throughout the year. On the mathematical side I would like to thank all the lecturers for this year with particular reference to Nick Biggs and Pete Chamberlain who help me a great deal through this project, cheers guys.

Finally I have to acknowledge all the people in 105 and thank them for a great year, a busy year but a great year nonetheless. And a special mention to the main motivational tool of the year - the 'I Don't Care!' sign.

Declaration

I confirm that this is my own work and the use of all material from other sources has been properly and fully acknowledged.

Signed.. Date..............

List of Figures

List of Tables

Chapter 1

Introduction

As a plane water-wave passes over a fixed underlying bed topography, part of the incident wave is reflected back and some is transmitted forward. This process is referred to as *wave scattering*.

Linear Wave Scattering by Topography

The governing equations are based on the fluid dynamics of the water, that is by assuming irrotation flow and using linearised boundary conditions for both the free surface and underlying topography, where we are concerned with motion in the (x, z) plane and consider the bed profile $h = h(x)$. Here z is chosen to point vertically upwards and x is a horizontal variable. This approach leads to a boundary value problem for the velocison va6onndv1(gra

Forward Wave Scattering

The *forward wave scattering* problem is concerned with finding the amplitude of the reflected and transmitted waves given that we know the amplitude of the incident wave, for any specified wave number $\nu = \omega^2/g$, where ω is the wave frequency and g is the acceleration due to gravity. In fact only the reflected wave amplitude need be found since the reflection and transmission coefficients are connected by certain identities.

To find the reflected wave amplitude $R(\nu)$ we assume that the bed topography, $h(x)$, is known and then use the shallow water and mild-slope approximations to formulate new boundary value problems (and equivalent integral equations). With the solution to these problems and the use of an appropriate substitution, $R(\nu)$ can be evaluated

Testing

It is not yet known whether the iteration process for solving the inverse scattering problem, in general, converges. For this reason we shall be testing both the inner and outer iterations to see if they do in fact converge, and if so whether this limit is the desired solution.

Chapter 2

Linear Wave Scattering by Topography

Before looking into the main problem of forward and inverse wave scattering by topography we first need to review some established work on wave scattering, as we will be using this work as a foundation to what follows.

2.1 Equations of Velocity Potential

If we consider the three dimensional case with depth z ,where $-h < z < 0$ and the bed profile $h = h(x, y)$, then we can formulate equations for the time-independent velocity potential $\varphi(x, y, z)$. By assuming that the flow is irrotational and by using linearised boundary conditions for the free surface of the water and bed topography, we have

$$\left.\begin{aligned} \nabla^2\varphi &= 0 \quad (-h < z < 0) \\ \varphi_z - \nu\varphi &= 0 \quad (z = 0) \\ \varphi_z + \nabla_h h \cdot \nabla_h \varphi &= 0 \quad (z = -h) \end{aligned}\right\}, \tag{2.1}$$

where $\nabla_h = (\partial/\partial x, \partial/\partial y)$ and $\nu = \omega^2/g$ with ω being the prescribed angular wave frequency and g the accelera z7.927usaue;

However we are not concerned with the full three-dimensional problem but a simpler case in which plane waves propagate parallel to the x-axis. This means we instead have $h = h(x)$ so that $\varphi = \varphi(x, z)$ and therefore separation of variables used on (2.1) gives

$$\varphi(x,z) = \left(A_0 e^{ikx} + B_0 e^{-ikx}\right) Z_0(z,h) + \sum_{n=1}^{\infty} \left(A_n e^{k_n x} + B_n e^{-k_n x}\right) Z_n(z,h), \tag{2.2}$$

on an interval where h is constant, for some constants A_n, B_n $(n \geq 0)$. Here,

$$\left.\begin{aligned} Z_0(z,h) &= c_0 \cosh k(z+h) \\ Z_n(z,h) &= c_n \cos k_n(z+h) \quad (n \geq 1) \end{aligned}\right\}, \tag{2.3}$$

where k denotes the positive real root of the dispersion relation

$$\nu = k \tanh kh \tag{2.4}$$

and k_n are the positive real roots of

$$\nu = -k_n \tan k_n h, \tag{2.5}$$

arranged such that $k_n < k_{n+1}$ for $n \geq 1$. We also have the coefficients (c_0, c_n) defined by

$$\begin{aligned} c_0 = c_0(h) &= 2\sqrt{k/(2kh + \sinh(2kh))}, \\ c_n = c_n(h) &= 2\sqrt{k_n/(2k_n h + \sin(2k_n h))}, \quad (n \geq 1), \end{aligned}$$

so that the functions $Z_n(z,h)$ $(n \geq 0)$ form a complete orthonormal set in the region $-h \leq z \leq 0$). There are also form a complete = z

2.1.1 Reflection and Transmission Coefficients

It is with these radiation conditions (2.6) that we can define the reflection and transmission coefficients from the scattering process that we will become more familiar with later. This is done by first choosing the direction of the incident wave.

For a wave incident from the left only we let $A_+ = 0$ and can define the reflection and transmission coefficients, R_- and T_- respectively, by

$$R_- = B_-/A_-, \quad T_- = B_+/A_-.$$

Similarly, by letting $A_- = 0$ describing waves incident from the right only, the corresponding reflection and transmission coefficients are

$$R_+ = B_+/A_+, \quad T_+ = B_-/A_+.$$

Using these two sets of coefficients we can easily define the the amplitudes $B_\pm$ of the outgoing waves relative to the incoming wave amplitudes $A_\pm$ by

$$\begin{pmatrix} B_- \\ B_+ \end{pmatrix} = S \begin{pmatrix} A_- \\ A_+ \end{pmatrix}, \quad S = \begin{pmatrix} R_- & T_+ \\ T_- & R_+ \end{pmatrix}, \tag{2.7}$$

where S here is the scattering matrix and can provide us with a description of the scattering process. There exist certain relationships between the scattering coefficents that were derived by Newman (1965), namely

$$\left.\begin{array}{c} |R_-|^2 + |T_+T_-| = |R_+|^2 + |T_+T_-| = 1 \\ \arg(T_-) = \arg(T_+) + 2\alpha_1\pi \\ \arg(R_+R_-) - \arg(T_+T_-) = \alpha_2\pi \end{array}\right\}, \tag{2.8}$$

where α_1 is an integer and α_2 is an odd integer. Another relation that g606F1511.97 -278(=)-A1411.995

to find $R_{\pm}$, therefore when performing calculations we only need concentrate on either the reflection or transmission coefficients.

2.2 Approximations of the Equations

Here the equations (2.1) are simplified by approximating the vertical structure of the fluid motion so as to remove the z coordinate, called ‘vertically integrated’ models. Approximations of this type have been derived using a variational principle.

Many variational principles have been given, but the form we shall use here is based on Porter and Staziker (1995) and also used by Porter and Chamberlain (1997).

2.2.1 Variational Approximation

Let D be a domain in the plane $z = 0$ with boundary C and define the functional

$$L(\psi) = \frac{1}{2} \iint_D \left\{ \nu(\psi^2)_{z=0} - \int_{-h}^{0} (\nabla\psi)^2 \right\} \mathrm{d}x\mathrm{d}y.$$

Let $\delta\psi$ denote an arbitrary variation of ψ, then the corresponding first variation of L is given by

$$\begin{aligned} \delta L = & \iint_D \Big\{ -(\delta\psi(\psi_z - \nu\psi))_{z=0} + (\delta\psi(\psi_z + \nabla_h h \cdot \nabla_h \psi))_{z=-h} \\ & + \int_{-h}^{0} \delta\psi \nabla^2\psi \mathrm{d}z \Big\} \mathrm{d}x\mathrm{d}y + \int_C \mathbf{n} \cdot \int_{-h}^{0} \delta\psi \nabla_h \psi \mathrm{d}z \mathrm{d}c \end{aligned}$$

where $\mathbf{n}$ is the outward normal unit vector on C. From this it follows that L is stationary for variations $\delta\psi$ which vanish on $C \times [-h, 0]$ if and only if $\psi = \varphi$, where φ satisfies (2.1) in $D \times [-h, 0]$.

An approximation to find the stationary point of L is done by restricting the choice of ψ to a particular class of functions. Since we are interested here in ‘vertically integrated’

$\delta L = 0$ with $\psi(x, y, z) = \xi(x, y)$ it follows that we have

$$ {}_h \cdot h \quad {}_h\xi + \nu\xi = 0, \tag{2.11}$$

which is the two-dimensional shallow water equation. We shall be using the one-dimensional version of this equation later where instead we have $\xi = \xi(x)$ and $h = h(x)$.

An alternative approximation can be found by instead choosing

ω

since we are only investigating a plane wave parallel to the x-axis, we shall be using the one-dimension version of (2.12) where $h = h(x)$ and $\varphi_0 = \varphi_0(x)$.

Chapter 3

Forward Wave Scattering

In this chapter we are concerned with finding the reflection coefficient, R, as defined in section 2.1.1. We will assume that we know the amplitude of the incident wave and also that we know the bed topography $h = h(x)$ for $x \in [0, l]$, and that

$$h(x) = \begin{cases} h_a & x < 0, \\ h_b & x > l, \end{cases} \tag{3.1}$$

where h_a and h_b are known constants, i.e. the depth at $x = 0$, $x = l$ can be measured. We also need to choose $\nu = \omega^2$

The particular problem that we shall be looking at is the case when we have a plane wave incident from the left, which is affected by the bed topography and causes both reflection and transmission waves as shown in Figure 3.1

3.1.1 Formulating the Problem

Using (3.2) and (3.3) we can formulate the boundary value problem

$$\left.\begin{aligned} \eta'' + k^2\eta &= 0 \qquad (0 < x < l) \\ \eta'(0) + ik_a\eta(0) &= 2ik_a \\ \eta'(l) - ik_a\eta(l) &= 0 \end{aligned}\right\}, \tag{3.4}$$

where we define $\eta = h\varphi'$. As shown by Chamberlain (1993), (3.4) can be formulated as the integral equation

$$\begin{aligned} \eta(x) &= e^{ik_a x} - \frac{i}{2k_a}\int_0^l e^{ik_a|x-t|}(k_a^2 - k^2(t))\eta(t)\mathrm{d}t, \\ &= e^{ik_a x} - \frac{i\nu}{2k_a}\int_0^l e^{ik_a|x-t|}\rho(t)\eta(t)\mathrm{d}t, \quad \rho(t) = \frac{1}{h_a} - \frac{1}{h(t)}. \end{aligned} \tag{3.5}$$

We note here that the lower and upper integration limits of (3.5) can be changed to $-\infty$ and ∞, since $\rho(t) = 0$ for $t < 0$, $t > l$.

Finally we need to rearrange the equations we have so that we can find R. To do this we consider

$$\eta(0) = h(0)\varphi'(0) = ik_a h_a I(1 - R),$$

then, without loss of generality, we choose $I = 1/ik_a h_a$ giving $\eta(0) = 1 - R$. Using this fact and (3.5) implies that

$$R = \frac{i\nu}{2k_a}\int_0^l e^{ik_a t}\rho(t)\eta(t)\mathrm{d}t = \frac{i\nu}{2k_a}\int_0^\infty e^{ik_a t}\rho(t)\eta(t)\mathrm{d}t. \tag{3.6}$$

We now have all that we need to solve the forward wave scattering process for shallow water. The procedure that we will follow is;

- Suppose the geometry of the problem is fixed, i.e. l and $h(t)$,
- Allow ν to vary in the chosen interval (ν_1, ν_2),
- For each ν, find η by solving either (3.4) or (3.5),

- Using η we can find $R = R(\nu)$ from (3.6).

It is important to note at this point that (3.5) and (3.6) can be conveniently written as

$$\eta(x) = e^{ik_a x} + (M(\rho)\eta)(x), \quad R(\nu) = (N(\eta)\rho)(\nu),$$

where we define the operators $M = M(\rho) : L_2(0, \infty) \to L_2(0, \infty)$ and $N = N(\eta) : L_2(0, \infty) \to L_2(0, \infty)$.

3.1.2 Difficulties For Large ν

Here we are concerned with knowing how R changes with ν, where we would expect that $|R| < 1$ and also that $|R| \to 0$ as $\nu \to \infty$ which can be seen in Figure 3.2. We expect $|R| < 1$ because this amplitude is relative to the incident wave, and the amplitude of the reflected wave should not be greater than that of the incident.

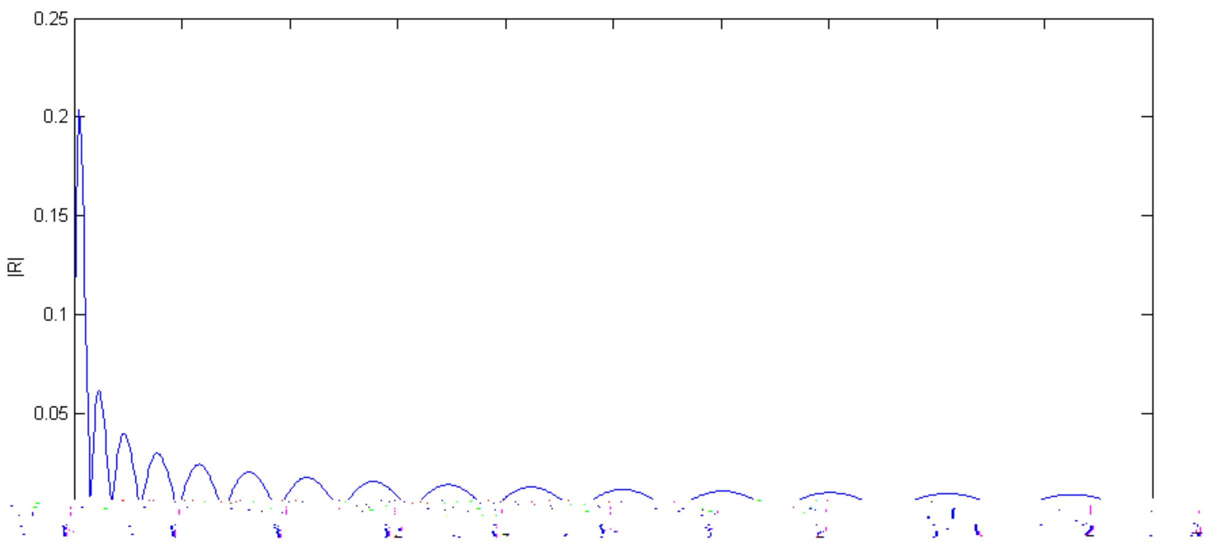

Figure 3.2: Plot of $|R(\nu)|$ using the shallow water approximation, where $l = 5$ and $h(x) = 0.2 - 0.05 \times \sin(2\pi x/5)$

We also expect $|R|$ to be small for large $\nu = \omega^2/g$ (where ω is wave frequency) because waves with large frequencies have small wavelengths, and hence would not be affected by the bed topography meaning there would be little to no reflection. However in this case, shallow water, it is not applicable to be talking about large ν since in the dispersion relation (2.4) we have assumed that $kh \ll 1$ implying that $\tanh kh \approx kh$. By taking ν to be large implies that k is large and hence this assumption is no longer valid.

Because it is not very accurate to use the shallow water approximation for large ν, we need to use a more accurate approximation so that talking about the behaviour of $|R|$ as $\nu \to \infty$ makes sense.

3.2 Mild-Slope Approximation

We now attempt to achieve greater accuracy by removing the restriction to shallow water. For this we look at the modified mild slope equation (2.12) for the one-dimensional case $\varphi_0 = \varphi_0(x)$ and $h = h(x)$, giving

$$(u_0\varphi_0')' + (k^2u_0 + h''u_1 + (h')^2u_2)\varphi_0 = 0,$$

where u_0,

3.2.1 Formulating the Problem

In a similar way as for the shallow water case, using (3.7) with (3.8) we can create the boundary problem

$$\eta'' + k^2\eta = 0 \qquad (0 < x < l)$$

For convenience later, we can write (3.10) and (3.11) as

$$\eta(x) = e^{ik_a x} + (P(\rho)\eta)(x), \qquad R(\nu) = (Q(\eta)\rho)(\nu)$$

respectively, where we define the integral operators $P = P(\rho) : L_2(0, \infty) \to L_2(0, \infty)$ and $Q = Q(\eta) : L_2(0, \infty) \to L_2(0, \infty)$.

3.2.2 The Behaviour of R

The forward scattering problem is concerned with the behaviour of R for $\nu \quad (\nu_1, \nu_2)$. What we would again expect is that $|R| < 1$ for all $\nu \quad (0, \infty)$, since a reflected wave should not have a greater amplitude than the incident wave. We would also expect that $|R| \to 0$ as $\nu \to \infty$, since waves of this type would be too small to be affected by the bed topography, and hence not reflect.

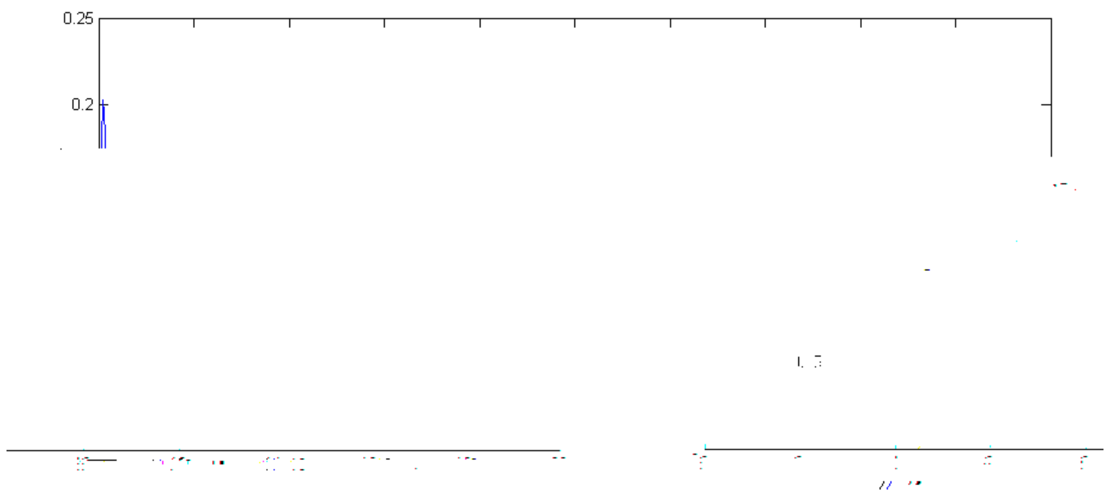

Figure 3.3: Plot of $|R(\nu)|$ using the mild-slope approximation, where $l = 5$ and $h(x) = 0.2 - 0.05 \times \sin(2\pi x/5)$

This expected behavior can be seen in Figure 3.3, but we notice that ν does not have to be that large for $|R|$ to be approximately equal to zero. This in fact appears to happen for $\nu \geq 11$ in this particular example.

$1/\sinh 2k_\theta h_\theta$ as $\nu \to \infty$. Therefore we see that, for large ν

$$|R| \approx e^{-2k_\theta h_\theta}. \tag{3.16}$$

3.3 Implementation

There are many ways in which this problem could be implemented. For example, (

MATLAB which gives a numerical solution using Runge Kutta 4 and 5 schemes.

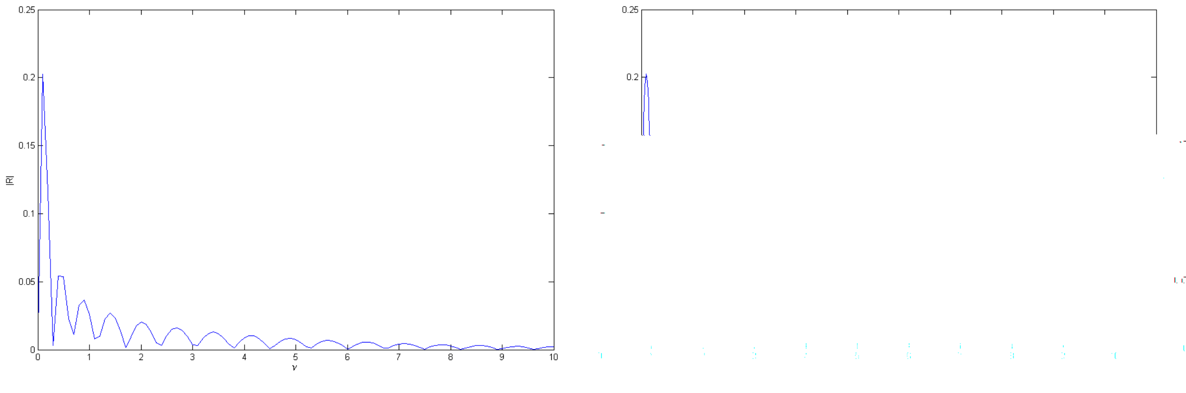

Figure 3.4: Plots of $|R(\nu)|$, where $l = 5$ and $h(x) = 0.2 - 0.05 \times \sin(2\pi x/5)$ with $M = 100$ and $M = 1000$ respectively

The domain x $[0, l]$, is divided into N equal sections using $(N + 1)$ nodes and the range of ν (ν_1, ν_2) is divided into M equal sections using $(M + 1)$ nodes. In this case we have set $N = 100$ and looked at the results of $|R|$ with different values of M.

In Figure 3.4 we can see that with $M = 100$, some of the information about R has been lost because the discretisation of (ν_1, ν_2) is not fine enough. Comparing this with the M

We can define $\eta = k^{-2}\varphi$

Chapter 4

Inverse Wave Scattering

In this chapter we are concerned with using given information about the reflection coefficient to approximate the bed topography, $h(x)$ for x $(0, l)$.

We shall assume that the reflection coefficient $R = R(\nu)$ for ν (ν_1, ν_2) and l are known, and that h_a, h_b can be measured and so also known, as shown in Figure 4.1.

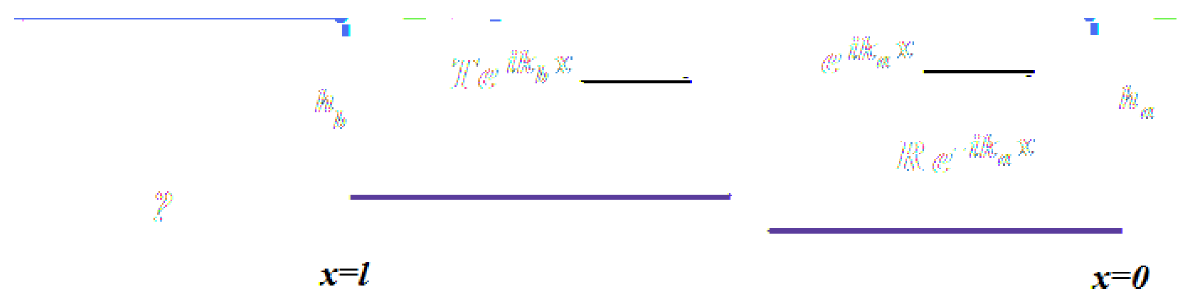

Figure 4.1: Graphical representation of the inverse scattering problem, where R and T are the reflection and transmission amplitudes respectively and $h(x)$, the quiescent depth, is to be found.

The procedure that we shall use to approximate $h(t)$ in this section is an iterative one, whereby if we have an approximation $h_n(t)$ to $h(t)$, we seek to improve this to $h_{n+1}(t)$ b where the inner iterations are used to converge each $h_n(t)$, and the outer iterations are used to get a first approximation to $h_{n+1}(t)$ from the converged value for $h_n(t)$.

4.1 Shallow Water Approximation

We will assume we have the simple case of $h_a = h_b$, and begin by looking at the shallow water case and suppose that we have an approximation $h_n(t)$ to $h(t)$. Then using the integral equation (3.5), given by $\eta(x) = e^{ik_a x} + (M(\rho)\eta)(x)$, we can define the n^{th} approximation to (3.5) by

$$\eta_n(x) = e^{ik_a x} - \frac{i\nu}{2k_a}\int_0^l e^{ik_a|x-t|}\rho_n(t)\eta_n(t)\mathrm{d}t, \quad \rho_n(t) = \frac{1}{h_a} - \frac{1}{h_n(t)}. \tag{4.1}$$

Then once we have solved this approximation for η_n we seek to solve

$$R(\nu) = \frac{i\nu}{2k_a}\int_0^l e^{ik_a t}\rho_{n+1}(t)\eta_n(t)\mathrm{d}t, \tag{4.2}$$

for $\rho_{n+1}(t)$, where $R(\nu)$ is known. Then it is a simple case of finding $h_{n+1}(t)$ given by

$$h_{n+1}(t) = \frac{h_a}{1 -+1}$$

$\eta_0(x) = e^{ik_a x}$. Therefore, using (4.2) gives

$$R(\nu) = \frac{i\nu}{2k_a}\int_0^\infty e^{2ik_a t}\rho_1(t)\mathrm{d}t, \tag{4.3}$$

which we wish to solve for $\rho_1(t)$. There are two ways that we can do this, either by inverting a sine, or cosine Fourier transform. If we take the real part of (4.3), we get

−Re50

sine transform (4.5) because it has the property that $\rho_1(0) = 0$, forcing us to have $h_1(0) = h_a$. We do not have this property with the Fourier cosine transform and so we may not necessarily match the first point $h_1(0)$ as accurately as possible.

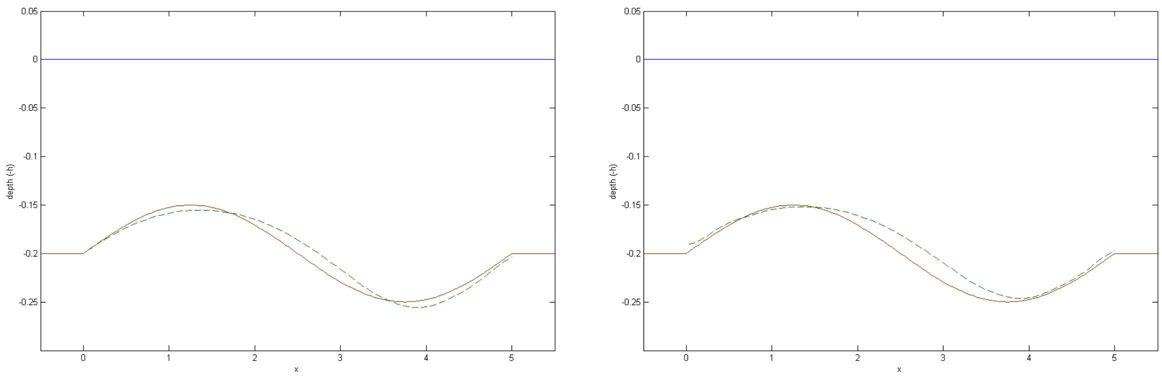

Figure 4.2: $h_1(t)$ (green) as found by (4.5) and (4.6) respectively to approximate bed topography (brown).

Expressions (4.5) and (4.6) are only practical if the integral on the right hand side can be reasonably approximated for $R(\nu)$ where $\nu \quad (\nu_1, \nu_2)$. This is related to the problem as noted earlier that the shallow water equations no longer make sense when we begin to talk about $\nu \to \infty$. The effect of this shall be investigated later.

Now that we have a first iterate $h_1(t)$, we can fully define the method for subsequent iterations.

4.1.2 Further Approximations - $h_{n+1}(t)$

Finding further approximations ,$h_{n+1}(t)$, to $h(t)$ requires a little more work than for the first approximation, $h_1(t)$, because the integral equation (4.2) is harder to deal with since we may not have that $\rho_n = 0$. The method that we shall use is to approximate each outer iterate, ρ_{n+1}, by an inner iteration.

We begin by noting that (4.1) can be written in the operator form $\eta_n(x) = e^{ik_a x} + (M(\rho_n)\eta_n)(x)$, as desribed in 3.1.1. Then using $h_n(t)$, we solve (4.1) for η_n and place this into (4.2) giving

$$\begin{aligned} R(\nu) &= \frac{i\nu}{2k_a}\int_0^l e^{ik_a t}\rho_{n+1}(t)(e^{ik_a t} + (M(\rho_n)\eta_n)(t))dt \\ &= \frac{i\nu}{2k_a}\int_0^l e^{2ik_a t}\rho_{n+1}(t)dt + \frac{i\nu}{2k_a}\int_0^l e^{ik_a t}\rho_{n+1}(t)(M(\rho_n)\eta_n)(t)dt, \end{aligned}$$

which we use to motivate the 'inner iteration'

$$\frac{i\nu}{2k_a}\int_0^l e^{2ik_a t}\rho_{n+1}^{(m+1)}(t)dt = R(\nu) - \frac{i\nu}{2k_a}\int_0^l e^{ik_a t}\rho_{n+1}^{(m)}(t)(M(\rho_n)\eta_n)(t)dt \qquad (4.7)$$

where we choose $\rho_{n+1}^{(0)} = \rho_n$. To recover $\rho_{n+1}^{(m+1)}$ from (4.7), as for the first approximation case, we can either invert a Fourier sine or cosine transform. For ease let us define

$$F^{(m)}(\nu) = R(\nu) - \frac{i\nu}{2k_a}\int_0^l e^{ik_a t}\rho_{n+1}^{(m)}(t)(M(\rho_n)\eta_n)(t)dt$$

so that using a Fourier sine transform gives

$$\rho_{n+1}^{(m+1)}(t) = -\frac{4}{h_a\pi}\int_0^\infty \frac{\mathrm{Re}(F^{(m)}(\nu))}{\nu}\sin(2\sqrt{\nu/h_a}t)d\nu. \qquad (4.8)$$

This is more desirable than using a Fourier cosine transform because we can see from (4.8) that we will always have $\rho_{n+1}(0) = 0$, and so for each approximation n we will have $h_n(0) = h_a$. If we suppose that some stopping criterion is met for the inner iteration when $m = M$ say, for some $M \geq 1$, then we have $\rho_{n+1} = \rho_{n+1}^{(M)}$ and hence can find $h_{n+1} = (h_a^{-1} - \rho_{n+1})^{-1}$.

The procedure that we then use, for the inverse wave s00.000.00RG1001-351.751-474

)when

Find $\rho_{n+1}^{(m+1)}$ from (4.8).

– Set $\rho_{n+1} = \rho_{n+1}^{(M)}$,

– Set $h_{n+1} = (h_a^{-1} - \rho_{n+1})^{-1}$.

Solving this equation is more complicated than for the shallow water case because $\rho_1(t)$ depends on ν, and hence we cannot use an inverse Fourier transform directly. Instead we can approximate any $\rho_n(t)$ by

$$\rho_n(t) = k_a^2 - k_n^2(t) \approx (h_a - h_n(t)) \left(2k\frac{\partial k}{\partial h} \right)_{h=h_a} = \frac{-4k_a^3(h_a - h_n(t))}{2k_a h_a + \sinh(2k_a h_a)}, \tag{4.12}$$

which we can place into (4.11). Then taking the real part gives

$$\mathrm{Re}(R(\nu)) = \frac{2k_a^2}{2k_a h_a + \sinh(2k_a h_a)} \int_0^l \sin(2k_a t)(h_a - h_1(t))\mathrm{d}t,$$

which we can invert using an inverse Fourier sine transform leading to

h

4.2.2 Further Approximations - $h_{n+1}(t)$

Finding further approximations, h

M

M

say, for some $M \geq 1$, then we have $h_{n+1} = h^{(M)}$

where

$$g(x_j) = e^{ik_a x_j} \qquad K(x_j, x_i) = -\frac{i}{2k_a} e^{ik_a|x_j - x_i|}\rho_n(x_i)$$

and σ_i are constants such that $\sigma_0 = \sigma_N = \Delta x/2$, and $\sigma_i = \Delta x$ for $i = 1, \cdots, N - 1$.

It is clear that (4.18) represents a system an $(N + 1)$ equations for the unknowns $\eta_n(x_j)$, $j = 0, \cdots, N$.

We introduce the vectors

$$\underline{\eta}_n = \begin{pmatrix} \eta_n(x_0) \\ \vdots \\ \eta_n(x_N) \end{pmatrix}, \qquad \underline{g} = \begin{pmatrix} g(x_0) \\ \vdots \\ g(x_N) \end{pmatrix},$$

and the matrix

$$K = \begin{pmatrix} K_{00} & K_{01} & \cdots & K_{0N} \\ \vdots & \vdots & & \vdots \\ K_{N0} & K_{N1} & \cdots & K_{NN} \end{pmatrix},$$

where $K_{ji} = \sigma_i K(x_j, x_i)$. Using these we can rewrite (4.18) and rearrange to find the solution vector, given as

$$\underline{\eta}_n = (I - K)^{-1}\underline{g}.$$

Once $\eta_n(x)$ has been approximated, we use a simple trapezium numerical method to estimate (4.17) in order to find $h^{(m+1)}_{n+1}$. The stopping criterion that we use is to look at the maximum difference between the $(m)^{\text{th}}$ and $(m-1)^{\text{th}}$ iteration given by

=m $\left\| h^{(m)}_{n+1} - h^{(m-1)}_{n+1} \right\|_\infty =$ K 004910Td[())]TF407.97Tf39051 will be investigated in Chapter 5.

4.4 A Possible Extension

What we have dealt with so far is the simple case where $h_a = h_b$. How can we change the inverse iteration process used for the simple case to solve the far more likely (and complicated) problem when $h_a = h_b$? We shall use the mild-slope approximation and suppose that we know $R = R(\nu)$ for $\nu \in (0, \infty)$. We will again be using an iterative process so we shall also suppose that we already have an approximation, $h_n(t)$, and are seeking an improvement, $h_{n+1}(t)$, to $h(t)$.

To begin, we let $k_n = k(h_n)$ be the solution to the dispersion relation (2.4) and then, based on (3.18), we solve the forward problem

$$\eta_n(x) = \gamma_n e^{ik_b x} - \frac{i}{2k_b}\int_0^l e^{ik_b|x-t|}(k_b^2 - k_n^2(t))\eta_n(t)\mathrm{d}t, \tag{4.19}$$

for η_n, where

$$\gamma_n = \frac{k_a}{k_b} + \frac{1}{2}\left(1 - \frac{k_a}{k_b}\right)\eta_n(0).$$

Combining (4.19) with (3.20), we aim to update our approximation to $h(t)$ by using

$$R(\nu) = \frac{k_b - k_a}{k_b + k_a} + \frac{i}{k_b + k_a}\int_0^\infty e^{ik_b t}(k_b^2 - k_{n+1}^2(t))\eta_n(t)\mathrm{d}t, \tag{4.20}$$

so that we can extract $k_{n+1}(t)$. Using this we can obtain $h_{n+1} = k_{n+1}^{-1}\tanh^{-1}(\nu k_{n+1}^{-1})$, and this will be referred to as the outer iteration. The inner iteration is concerned with extracting k_{n+1} from (4.20).

Using (4.19) we can write $\eta_n(t) = \gamma_n e^{ik_b t} + (\eta_n(t) - \gamma_n e^{ik_b t})$, then placing this into

$h_0(x) = h_b$ so that (4.19) simplifies to give $\eta_0(x) = \gamma_n e^{ik_b x}$.x Using this ie83b

Chapter 5

Results

In this section we are going to test certain aspects of the inverse scattering iteration process as described in Chapter 4. We shall look at how accurate the shallow water and mild-slope approaches are with respect to estimating each approximation to $h(x)$, $h_n(x)$, and we shall also test the convergence of the inner and outer iterations.

The depth profiles that we shall be using are;

- $h_A(x) = h_a - \ \sin(\frac{2\pi x}{l})$, where we shall choose $h_a = 0.2$, $= 0.02$ and $l = 5$.

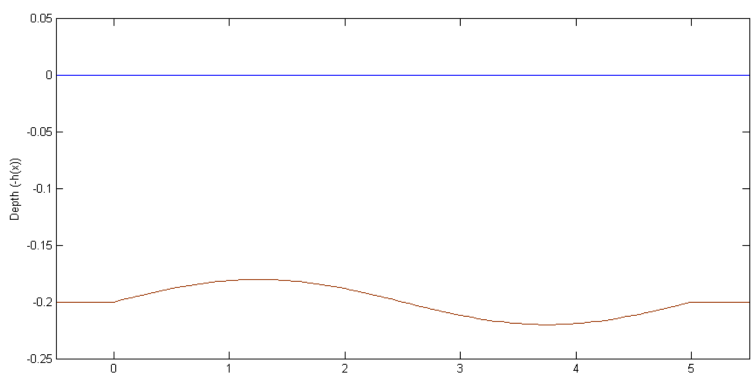

Figure 5.1: Depth profile $h_A(x)$.

- $h_B(x) = h_a\ 1 + 2\ \ 1 - \ ((x/l) - \alpha) \cdot \frac{(x/l)-1+\alpha}{\alpha(1-\alpha)}\ ^2$, where we shall choose h_a = 0.2, = 0.05, $\alpha = 0.15$ and $l = 5$.

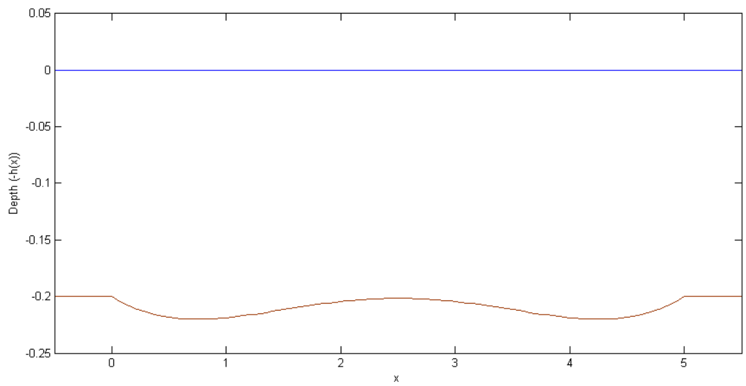

Figure 5.2: Depth profile $h_B(x)$.

- $h_C(x) = h_a(1 + \ \sin(2\pi(x/l)^4) - 0.5\ \ \sin(2\pi((l-x)/l)^4))$, where we shall choose $h_a = 0.2$, = 0.08 and $l = 5$.

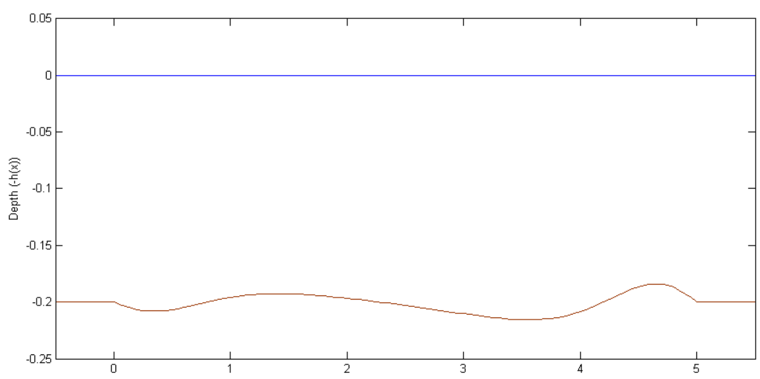

Figure 5.3: Depth profile $h_C(x)$.

To be able to test the procedure we have formulated to solve the inverse problem we first need to find $R(\nu)$ for $\nu\ \ (\nu_1, \nu_2)$. We do this by setting the depth profile, $h(x)$ for

x $(0, l)$, choose the range $(\nu_1, \nu$

error between $h(x)$ and $h_1(x)$ varies with the range of ν, and for each bed topography h_A, h_B, h_C. We can see that these errors are not large, but there is still much room for improvement.

	h_A		h_B		h_C	
ν_2	$\frac{\|h-h_1\|_\infty}{\|h\|_\infty}$	$h - h_1 \ {}_2$	$\frac{\|h-h_1\|_\infty}{\|h\|_\infty}$	$h - h_1 \ {}_2$	$\frac{\|h-h_1\|_\infty}{\|h\|_\infty}$	$h - h_1 \ {}_2$
0.1	0.0786	0.0472	0.0677	0.0849	0.0812	0.0762
0.2	0.0386	0.0125	0.0536	0.0368	0.0635	0.0645
0.4	0.0282	0.0114	0.0395	0.0233	0.0404	0.0385
0.6	0.0195	0.0115	0.0377	0.0164	0.0353	0.0371
0.8	0.0191	0.0113	0.0359	0.0162	0.0329	0.0196
1	0.0159	0.0113	0.0364	0.0159	0.0292	0.0204
2	0.0123	0.0108	0.0323	0.016	0.0204	0.0121
4	0.0127	0.0108	0.0295	0.0168	0.0125	0.0076
6	0.0145	0.0112	0.0268	0.018	0.0093	0.0067
8	0.0159	0.0119	0.0241	0.0198	0.0093	0.0065
10	0.0186	0.013	0.0214	0.0225	0.0093	0.0064
12	0.0205	0.0143	0.0209	0.0258	0.0093	0.0064
14	0.0223	0.0156	0.0236	0.0295	0.0093	0.0065
16	0.0245	0.017	0.0259	0.0335	0.0093	0.0067
18	0.0268	0.0184	0.0286	0.0376	0.0097	0.007
20	0.0291	0.0195	0.0309	0.0416	0.0107	0.0073

Table 5.1: Error analysis of $h_1(x)$ as an approximation to $h(x)$ using the shallow water approximation.

We notice that from these results that the smallest values, $\nu_2 = 0.1$, $\nu_2 = 0.2$ give much larger errors, which may be because we have not included enough information from $R(\nu)$20.7937T1391.0955 0 Tf13 F3 11.95528353(b)-2802027

5.1.2 Mild-Slope Approximation

As for the shallow water approximation, we are fixing $\nu_1 = 0.0001$ and allowing ν_2 $[0.1, 20]$, then approximating (4.13) between these limits $(\nu_1, \nu_2)^2$. Also, as before, we have set $N = 100$ and $M = 1000$. Therefore we are setting $\Delta x = l/100$ and giving a variable $\Delta \nu$.

The results from finding the error between the first approximation, $h_1(x)$ found using (4.13), and the actual bed topography, $h(x)$, for different ranges of ν are shown in Table 5.2 .

	h_A		h_B		h_C	
ν_2	$\frac{\|h-h_1\|_\infty}{\|h\|_\infty}$	$h - h_1$ $_2$	$\frac{\|h-h_1\|_\infty}{\|h\|_\infty}$	$h - h_1$ $_2$	$\frac{\|h-h_1\|_\infty}{\|h\|_\infty}$	$h - h_1$ $_2$
0.1	0.0464	0.0449	0.0695	0.0881	0.0812	0.0762
0.2	0.0232	0.0187	0.0386	0.0397	0.0631	0.0648
0.4	0.0136	0.0143	0.0286	0.0276	0.0390	0.0379
0.6	0.0109	0.0138	0.0236	0.0187	0.0348	0.0349
0.8	0.0100	0.0137	0.0264	0.0198	0.0315	0.0191
1	0.0095	0.0137	0.0255	0.0186	0.0292	0.0190
2	0.0105	0.0142	0.0282	0.0189	0.0181	0.0098
4	0.0114	0.0159	0.0323	0.0220	0.0102	0.0077
6	0.0123	0.0181	0.0359	0.0262	0.0088	0.0075
8	0.0136	0.0206	0.0395	0.0311	0.0093	0.0078

what we would expect as a result of the mild-slope approximation, and so a possible reason for this problem may be that in our numerical evaluation of (4.13) we are using a variable $\Delta\nu$. If instead we used a fixed $\Delta\nu$ and a variable M we may get better accuracy, which we shall test later.

5.2 Convergence of Iterations

Once a first approximation has been calculated, the inverse scattering process is an iterative one but it is not yet known whether these iterations will converge to the solution $h(x)$. Therefore in this section we are testing the convergence of this iterative process using (4.8) and (4.17), for shallow water and mild slope approximations respectively.

To test for inner iteration convergence we are looking at the maximum error between the $(m)^{\text{th}}$ and $(m-1)^{\text{th}}$ iterates given by

$$\|h_n^{(m)} - h_n^{(m-1)}\|_\infty = \max_{j=0,\cdots,N} |h_n^{(m)}(x_j) - h_n^{(m-1)}(x_j)|,$$

and similarly for outer iteration convergence we are looking at the maximum error between the $(n)^{\text{th}}$ and $(n-1)^{\text{th}}$ iterates given by

$$\|h_n - h_{n-1}\|_\infty = \max_{j=0,\cdots,N} |h_n(x_j) - h_{n-1}(x_j)|,$$

where we have discretised $h_n(t)$ using $(N+1)$ nodes, and $x_j = j\Delta x$ where $\Delta x = l/N$. For convergence we expect this value to be very small, and decrease to zero as m and n are increased.

We shall also be testing to see if this new approximation, $h_n(x)$, has actually converged to the solution, $h(x)$, that we are looking for, since it may converge to an entirely wrong approximation. To test for this we shall be using the same error norms as used to test the accuracy of the first approximation, $h_1(x)$, and we shall be comparing these to the first approximation in order to ascertain whether this new approximation is more accurate.

5.2.1 Shallow Water Approximation

As for the first approximation, we have found $R(\nu)$ for ν (ν_1, ν_2) where we have set ν_1

	h_A		h_B		h_C	
ν_2	$\frac{\|h-h_1\|_\infty}{\|h\|_\infty}$	$\frac{\|h-h_2\|_\infty}{\|h\|_\infty}$	$\frac{\|h-h_1\|_\infty}{\|h\|_\infty}$	$\frac{\|h-h_2\|_\infty}{\|h\|_\infty}$	$\frac{\|h-h_1\|_\infty}{\|h\|_\infty}$	$\frac{\|h-h_2\|_\infty}{\|h\|_\infty}$
0.5	0.0232	0.0295	0.0423	0.0605	0.0366	0.0533
1	0.0159	0.0550	0.0364	0.1114	0.0292	0.1257
5	0.0132	1	0.0282	1	0.0102	1.0264

Table 5.5: Comparing the relative error of $h_1(x)$ with $h_2(x)$.

	h_A		h_B		h_C	
ν_2	$h - h_1 \;{}_2$	$h - h_2 \;{}_2$	$h - h_1 \;{}_2$	$h - h_2 \;{}_2$	$h - h_1 \;{}_2$	$h - h_2 \;{}_2$
0.5	0.0124	0.0327	0.0199	0.044	0.0371	0.0535
1	0.0113	0.048	0.0159	0.0908	0.0204	0.1186
5	0.011	2.005	0.0173	2.1137	0.007	0.4691

Table 5.6: Comparing the total error of $h_1(x)$ with $h_2(x)$.

the correct solution we would expect this new approximation to be more accurate than the previous.

In Tables 5.5 and 5.6 we have compared the accuracy of $h_2(x)$ with $h_1(x)$ in approximating $h(x)$. We can see from the results shown that the new approximation is less accurate than the first approximation, in fact we can see that as ν_2 is increased the errors have become very large. From this we can infer that the iteration process fails

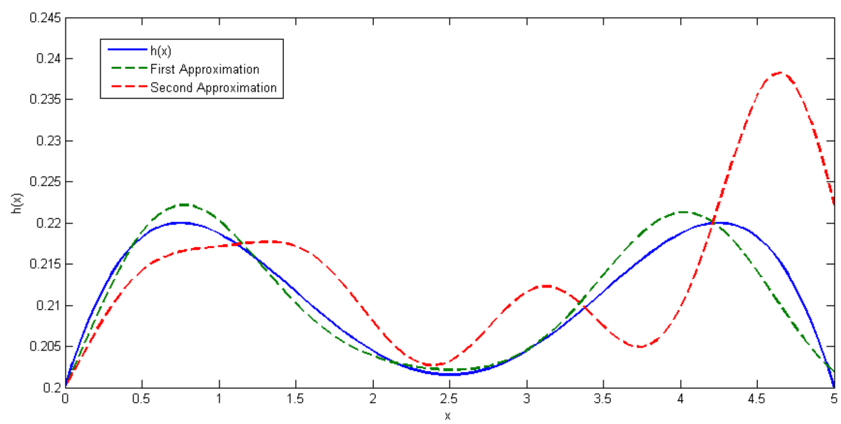

Figure 5.4: Comparis4Td[]r50Td[]615063Tf12.2420Td[(h)]TJ6.94Tf5.74-1.49Td[(1)]T5.76.7500351.7500cm

Even though the iterations appear to be convergent, we cannot guarantee that what they are converging to is the required solution. To test this we have performed similar error analysis as with the first approximation, the results of which can be seen in Table 5.8. The results show that the approximations, $h_n(x)$, are more accurate for smaller values of ν_2 and that the errors become much larger as ν_2 is increased, which is most likely as a result of the restriction to shallow water.

---

even though ν_2 gives the smallest errors, the converged solution is a poor approximation to $h(x)$. This is possibly most clear for the case when $h = h_C$.

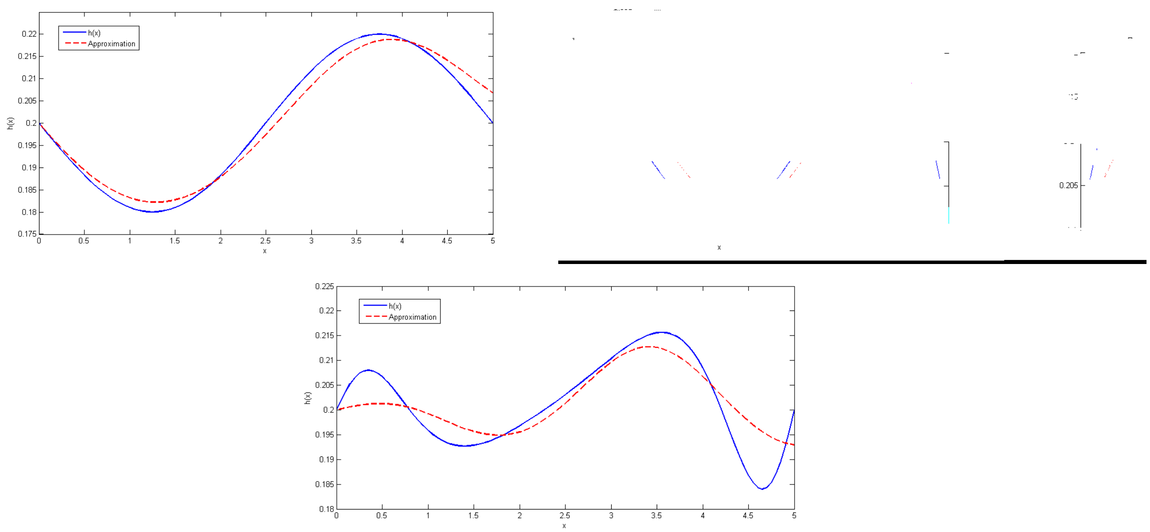

Figure 5.5: Converged depth profiles for h_A, h_B and h_C respectively with $\nu_2 = 0.3$, using the shallow water approximation.

5.2.2 Mild-Slope Approximation

As for the shallow water approximation, we have found $R(\nu)$ for ν (ν_1, ν_2) where we have set $\nu_1 = 0.0001$ and allowed ν_2 to vary. In each case, for numerical computation, we have uniformly discretised ν using $(M + 1)$ nodes meaning that $\Delta\nu = (\nu_2 - \nu_1)/M$ is variable, as earlier.

Inner Iterations

From Tables 5.9 and 5.10 we can see that the inner iterations appear to be converging as the number of iterations, m, is increased. Also by comparing Tables 5.9 and 5.10 with 5.3 and

	$h_2^{(m)} - h_2^{(m-1)} \quad {}_{\infty}$		
m	h_A	h_B	h_C
2	1.68×10^{-4}	1.30×10^{-4}	2.93×10^{-6}
3	1.40×10^{-5}	8.38×10^{-6}	2.47×10^{-8}
4	8.04×10^{-7}	5.59×10^{-7}	2.73×10^{-10}
5	6.79×10^{-8}	3.96×10^{-8}	2.55×10^{-12}
10	7.82×10^{-14}	5.07×10^{-14}	0

	h_A		h_B		h_C	
ν_2	$\frac{\|h-h_1\|_\infty}{\|h\|_\infty}$	$\frac{\|h-h_2\|_\infty}{\|h\|_\infty}$	$\frac{\|h-h_1\|_\infty}{\|h\|_\infty}$	$\frac{\|h-h_2\|_\infty}{\|h\|_\infty}$	$\frac{\|h-h_1\|_\infty}{\|h\|_\infty}$	$\frac{\|h-h_2\|_\infty}{\|h\|_\infty}$
0.5	0.0127	0.0118	0.0259	0.0241	0.0343	0.0348
1	0.0095	0.0114	0.0255	0.0150	0.0292	0.0311
5	0.0118	0.0127	0.0345	0.0209	0.0083	0.0097
10	0.0150	0.0150	0.0432	0.0373	0.0088	0.0083
15	0.0186	0.0191	0.0532	0.0523	0.0102	0.0102

Table 5.12: Comparing the relative error of $h_1(x)$ with $h_2(x)$.

	h_A		h_B		h_C	
ν_2	$h - h_1$ $_2$	$h - h_2$ $_2$	$h - h_1$ $_2$	$h - h_2$ $_2$	$h - h_1$ $_2$	$h - h_2$ $_2$
0.5	0.0142	0.014	0.0243	0.021	0.0363	0.0362
1	0.0137	0.0136	0.0186	0.0134	0.019	0.0182
5	0.0169	0.0168	0.024	0.019	0.0076	0.0069
10	0.0233	0.0232	0.0366	0.0333	0.0081	0.0075
15	0.0301	0.0301	0.0513	0.0491	0.0094	0.0089

Table 5.13: Comparing the total error of $h_1(x)$ with $h_2(x)$.

Tables 5.12 and 5.13 show the errors between the newly converged $h_2(x)$ and $h(x)$, compared with the error that arose using the first approximation. These results hint at the idea that the new approximation is more accurate than the first, and so the converged limit is in fact tending to the solution $h(x)$.

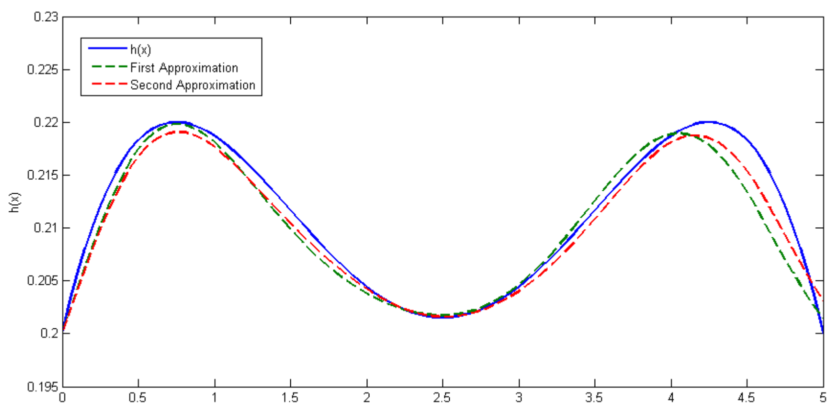

Figure 5.6: Comparison of h_1 with h_2 using $h = h_B$ and $\nu_2 = 1$.

This certainly appears to be the case when using $h = h_B$ since both the relative and total errors have decreased, and comparing Figure 5.6 with Figure 5.4 it is clear to see that the mild-slope approximation is working much accurately than the shallow water approximation. However, it is less clear that the inner iterations are converging to $h(x)$ for $h = h_A$ and $h = h_C$, since although some of the total errors may have decreased there are some instances where the the maximum error has increased. This is not the desired result, as we would hope to see the maximum error between $h_n(x)$ and $h(x)$ to tend to zero as n is increased.

Outer Iterations

As we did for the shallow water approximation, we now look at the outer iteration process for the mild-slope approximation and attempt to find signs that these iterates are converging and if so, to what solution. From Table 5.14 we can see that the maximum error between the (n^{th}) F400reased

Tables 5.14 and 5.7 we see that the convergence in the mild-slope approximation case, in general, is much faster and more convincing than in shallow water case. However, we still have the same question as to whether these iterations are in fact converging to the required solution $h(x)$.

In Table 5.15 we can see that the errors between the approximation, $h_n(x)$, and $h(x)$ do not grow or oscillate as in the shallow water approximation case. We also note that most of these errors are smaller than for the corresponding first approximation as shown in Table 5.2, and others are not greatly larger. This was not the case for the shallow water approximation, and so we can see that for the mild-slope approximation the iteration process appears to improving toward the desired solution.

		h_A		h_B		h_C	
ν_2	n	$\frac{\|h-h_n\|_\infty}{\|h\|_\infty}$	$\|h-h_n\|_2$	$\frac{\|h-h_n\|_\infty}{\|h\|_\infty}$	$\|h-h_n\|_2$	$\frac{\|h-h_n\|_\infty}{\|h\|_\infty}$	$\|h-h_n\|_2$
1	2	0.0114	0.0136	0.0150	0.0134	0.0311	0.0182
	3	0.0114	0.0137	0.0150	0.0137	0.0311	0.0182
	4	0.0114	0.0137	0.0155	0.0138	0.0311	0.0182
	5	0.0114	0.0137	0.0155	0.0138	0.0311	0.0182
5	2	0.0127	0.0168	0.0209	0.019	0.0097	0.0069
	3	0.0132	0.0169	0.0182	0.019	0.0102	0.0068
	4	0.0132	0.0169	0.0182	0.019	0.0102	0.0068
	5	0.0132	0.0169	0.0182	0.019	0.0102	0.0068
15	2	0.0191	0.0301	0.0523	0.0491	0.0102	0.0089
	3	0.0191	0.0302	0.0505	0.049	0.0102	0.0089
	4	0.0191	0.0302	0.0500	0.049	0.0102	0.0089
	5	0.0191	0.0302	0.0500	0.049	0.0102	0.0089

Table 5.15: Error analysis of $h_n(x)$ to $h(x)$ using the mild-slope approximation.

The greater accuracy in the mild-slope approximation over that of the shallow water approximation can also be seen by comparing Figure 5.7 with Figure 5.5 (and also in further results in Appendix A). Here we see that, particularly for at points where $h(x)$ has a local maximum or minimum. It is also possible that the amplitudes of these curves play a part in the accuracy of the approximation, since the turning points in $h = h_C$, that have smaller amplitude, are better approximated than those in $h = h_A$ or $h = h_B$.

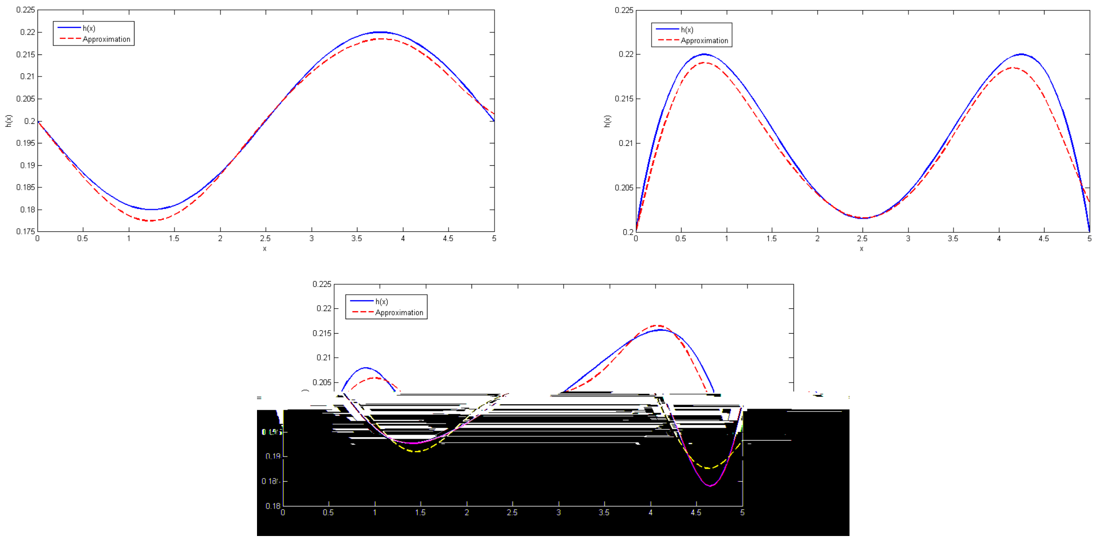

Figure 5.7:

5.3.1 Greater Accuracy?

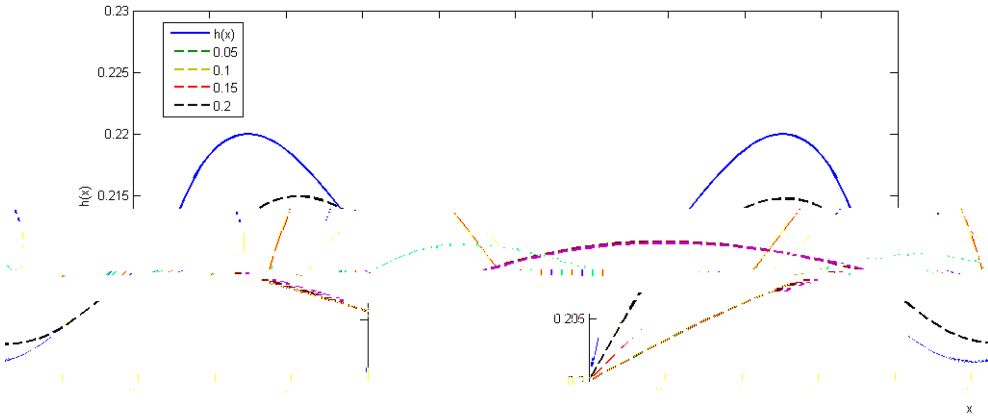

Figure 5.10: Converged depth profiles for $h = h_B$ using the mild-slope approximation, where ν_2 has been allowed to vary.

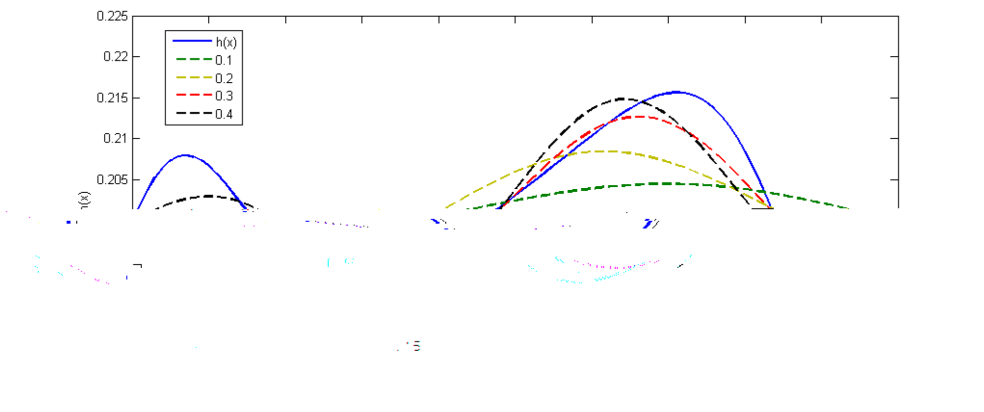

Figure 5.11: Converged depth profiles for $h = h_C$ using the mild-slope approximation, where ν_2 has been allowed to vary.

This level of accuracy for small ν is not shared in each case. For example, in Figure 5.10 with $h = h_B$, we can see that for ν $(0.0001, 0.2)$ the converged solution gives a very crude idea as to the topography, but not yet as accurate as for $h = h_A$. Also for more complicated topographies, as in Figure 5.11 with $h = h_C$, we see that a much larger range for ν is required, since for ν $(0.0001, 0.4)$ the converged solution is only just starting to take the shape of the actual solution.

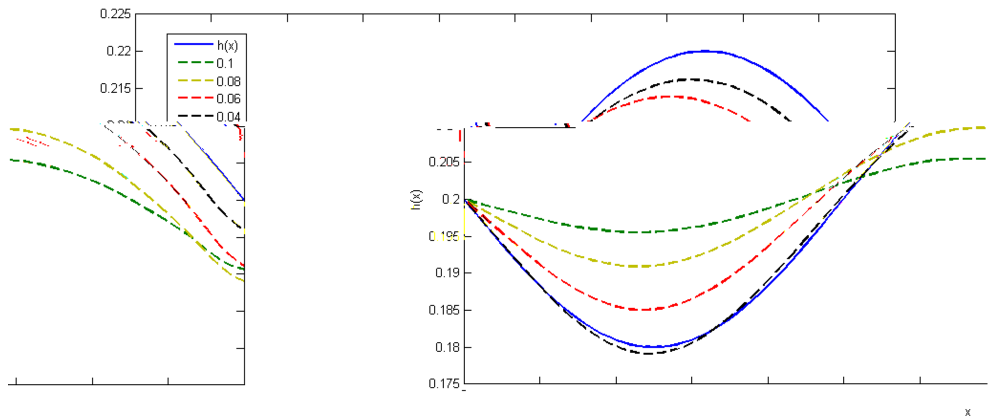

Figure 5.12: Converged depth profiles for $h = h_A$ using the mild-slope approximation, where ν_1 has been allowed to vary.

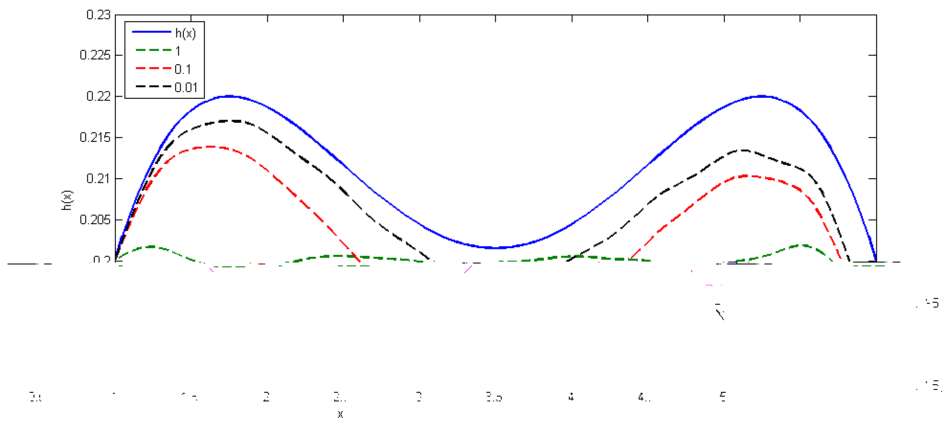

Figure 5.13: Converged depth profiles for $h = h_B$ using the mild-slope approximation, where ν_1 has been allowed to vary.

We are also interested to see how the converged approximation reacts if the smallest values of ν are no longer included. So far we have set $\nu_1 = 0.0001$ and allowed ν_2 to vary, here we shall instead fix83(0)]TF3911.955tere we sha496(also)-vs.0001 instead

From Figures 5.12, 5.13 and 5.14 we can see that this does indeed appear to be the case and furthermore, that for ν (1, 5) the approximations are particularly poor which is an indication that much of the necessary information is in the range (0, 1).

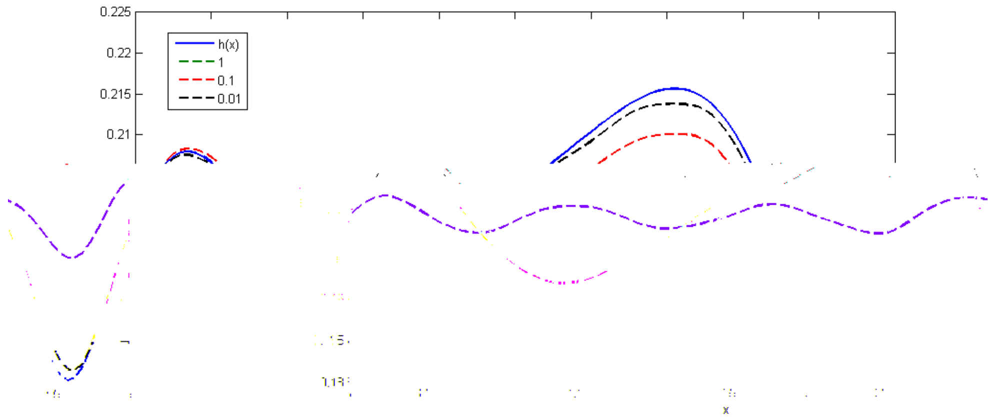

Figure 5.14:

By making the amplitude of these stationary points larger we expect that the errors will increase, and perhaps that the mild-slope approximation may fail to converge. In Figure 5.15 we can see that with a greater amplitude (half of the depth), the approximation is worse. The first approximation appears to be a fair estimate, but as soon as we begin the iterative process we see that the approximation is wildly inaccurate. Not only have the errors grown substantially but according to the approximation, the bed topography protrudes out of the water's surface.

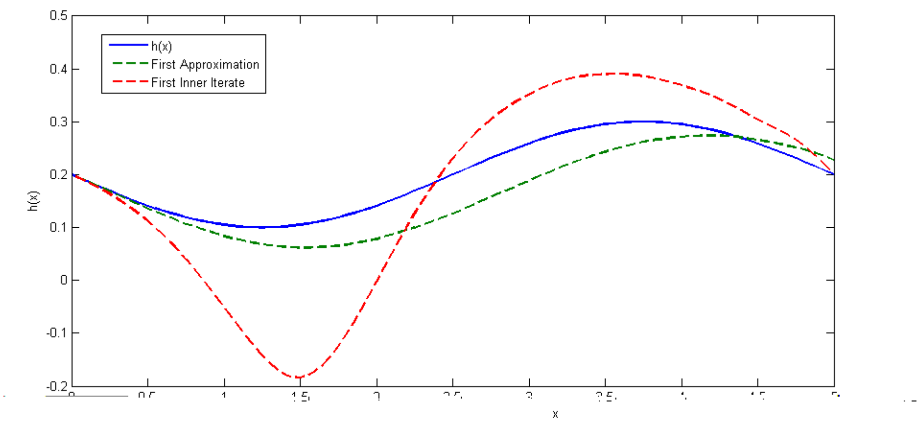

Figure 5.15: Depth profile $h = h_A$ with $= 0.1$

Conversely, by making the amplitude of stationary points smaller we get a much more accurate approximation. This is what we would expect since the mild-slope approximation is based on the idea that the gradient is very small and to have a stationary point of lesser amplitude means that the gradient is also less, and so the approximation works better.

Chapter 6

Summary, Future Work & Conclusions

Summary

In some existing literature on linear wave scattering, fundamental ideas of fluid dynamics were used to formulate a boundary value problem for the velocity potential of the water in the (x, z) plane. The solution to this could then be approximated, for simplicity, by using either the shallow water hypothesis that the wavelength is much greater than the quiescent depth, or by using the mild-slope hypothesis that the gradient of the underlying bed topography is small. Reflection and transmission coefficients were also defined for plane waves and had been found to rely on the amplitude of the incident wave. Also, through the use of an identity it was shown that knowing one of these coefficients meant the other could be recovered.

Using this theory and each approximation in turn, we were able to formulate a forward wave scattering problem. We assumed that the bed topography was known along with the amplitude of the incident wave and we were seeking the reflected amplitude, $R(\nu)$ for all ν $(0, \infty)$, where $\nu = \omega^2/g$ (with ω being the frequency of the incident wave, and g the acceleration due to gravity). This turned out to be fairly simple and we were able to find an explicit expression for $R(\nu)$. We then looked at the behaviour of R as $\nu \to \infty$ and found that for the shallow water approximation R did not tend to zero as was expected, which may have been due to large ν corresponding to wavelengths in some way on the norm of the integral operator in (4.9), which in turn is dependent on $h(x)$.

An evident problem with the inverse method is that without prior knowledge of the underlying topography, we have no way of knowing how accurate any given approximation results in Section 5.3.1, since we have also seen that including larger values of ν may not increase accuracy and so may be neglected. The accuracy of the approximation however, is also dependent on the amplitude of any stationary points in the bed profile, $h(x)$. The smaller the amplitude, the greater the accuracy meaning that to know our results are accurate we must already know that the gradient of the bed profile is very mild.

Therefore with a small range of reflected data, $R(\nu)$, and some prior knowledge that the bed profile is mild, we can use the iterative inverse method and mild-slope approximation to find an accurate representation of the underlying topography.

Appendix A

More Tables And Figures

A.1 Shallow Water Approximation

Inner Iteration Convergence

Following on from the results for the inner iteration convergence in Section 5.2.1, Tables A.1, A.2 and A.3 show the error between iterations for a larger range of ν (ν_1, ν_2). These results do not imply convergence to the solution.

	$h_2^{(m)} - h_2^{(m-1)}{}_{\infty}$		
m	h_A	h_B	h_C
2	0.0678	1.8175	0.3929
3	0.1135	9.0984	0.3124
4	10.9085	68.3473	0.2286
5	27.8077	68.1714	0.1371
10	0.731	0.0186	0.2667
15	0.0015	3.	

	$h_2^{(m)} - h_2^{(m-1)} \;{}_{\infty}$		
m	h_A	h_B	h_C
2	6.9635	84.6378	10.7729
3	8.9364	6.7553	10.5104
4	9.1073	0.7272	18.9734
5	1.4282	0.1739	19.2164
10	1.78×10^{-5}	9.26×10^{-8}	0.8124
15	1.38×10^{-9}	6.92×10^{-12}	2.70×10^{-4}

Table A.2: Maximum error between the $(m)^{th}$ and $(m-1)^{th}$ iterate with $\nu_2 = 10$, using the shallow water approximation.

	$h_2^{(m)} - h_2^{(m-1)} \;{}_{\infty}$		
m	h_A	h_B	h_C
2	93.2334	13.445	6.4016
3	92.9916	4.1052	22.7819
4	1.1235	1.0531	22.8502
5	0.0614	0.0103	0.6481
10	5.62×10^{-8}	7.87×10^{-9}	1.46×10^{-4}
15	1.66×10^{-14}	6.56×10^{-15}	9.97×10^{-8}

Table A.3: Maximum error between the $(m)^{th}$ and $(m-1)$

and A.2 are the converged limits for $h = h_A$ and $h = h_B$ respectively. It is also clear from these figures that the second iterate is not converging to the solution $h(t)$.

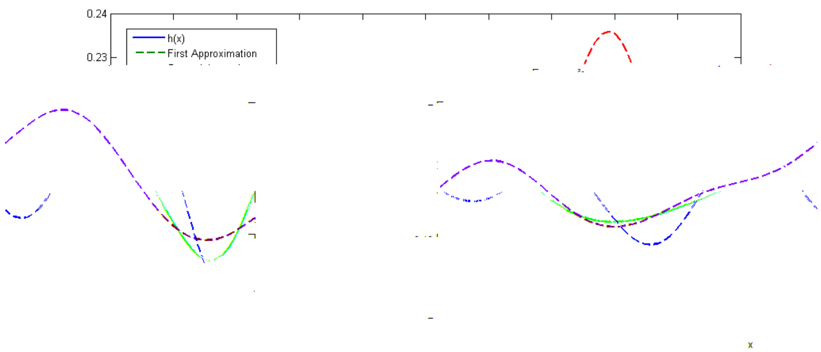

Once inner iteration convergence was established we moved on to the outer iteration convergence for the shallow water approximation, and concentrated on small values for ν_2. Following on from the results given in Section 5.2.2, Figures A.3 and A.4 show the converged approximations to $h(x)$ for other ranges of ν.

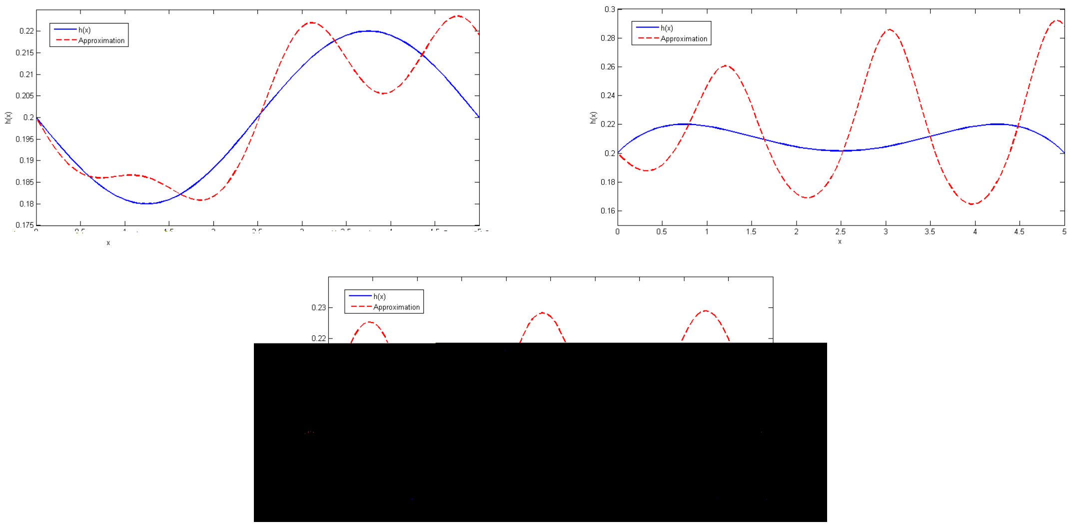

Figure A.4: Converged depth profiles for h_A, h_B and h_C respectively with $nu_2 = 0.7$, using the shallow water approximation.

A.2 Mild-Slope Approximation

Inner Iteration Convergence

Following on from the results for the inner iteration convergence in Section 5.2.2, Tables A.4 and A.5 show the error between iterations for different ranges of ν (ν_1, ν_2). These results help to reinforce the implication that inner iterations are converging using the mild-slope approximation. As was noted in Section 5.2.2 the convergence for the mild-

	$h_2^{(m)} - h_2^{(m-1)}\ {}_{\infty}$		
m	h_A	h_B	h_C
2	2.43×10^{-4}	6.50×10^{-4}	1.14×10^{-4}
3	2.97×10^{-5}	2.00×10^{-4}	9.00×10^{-6}
4	5.39×10^{-6}	4.41×10^{-5}	7.98×10^{-7}
5	8.77×10^{-7}	1.31×10^{-5}	6.69×10^{-8}
10	8.81×10^{-10}	1.86×10^{-8}	2.91×10^{-13}
15	1.93×10^{-12}	3.24×10^{-11}	2.78×10^{-17}

Table A.4: Maximum error between the $(m)^{th}$ and $(m-1)^{th}$ iterate with $\nu_2 = 5$, using the mild-slope approximation.

	$h_2^{(m)} - h_2^{(m-1)}\ {}_{\infty}$		
m	h_A	h_B	h_C
2	2.68×10^{-4}	7.39×10^{-4}	1.13×10^{-4}
3	3.34×10^{-5}	1.39×10^{-4}	7.79×10^{-6}
4	6.21×10^{-6}	4.01×10^{-5}	7.95×10^{-7}
5	1.12×10^{-6}	5.07×10^{-6}	6.53×10^{-8}
10	1.19×10^{-9}	1.05×10^{-8}	6.00×10^{-13}
15	4.26×10^{-12}	1.16×10^{-11}	2.78×10^{-17}

Table A.5: Maximum error between the $(m)^{th}$ and $(m-1)^{th}$ iterate with $\nu_2 = 15$, using the mild-slope approximation.

slope approximation appears to faster than for the shallow water approximation. This is quite evident by comparing Tables A.4 and A.5 with Tables A.1, A.2 and A.3 as the errors for the mild-slope approximation are smaller and decrease faster as m is increased.

It is also evident, by simply comparing Figures A.5 and A.6 with Figures A.1 and A.2, that the mild-slope approximation produces far more accurate second iterates, $h_2(x)$, than the shallow water approximation.

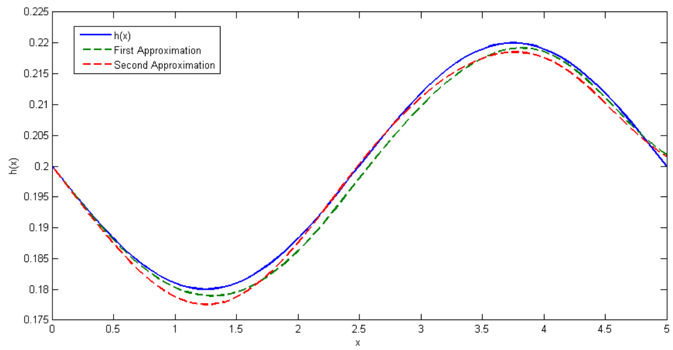

Figure A.5: Comparison of h_1 with h_2 using $h = h_A$ and $\nu_2 = 1$.

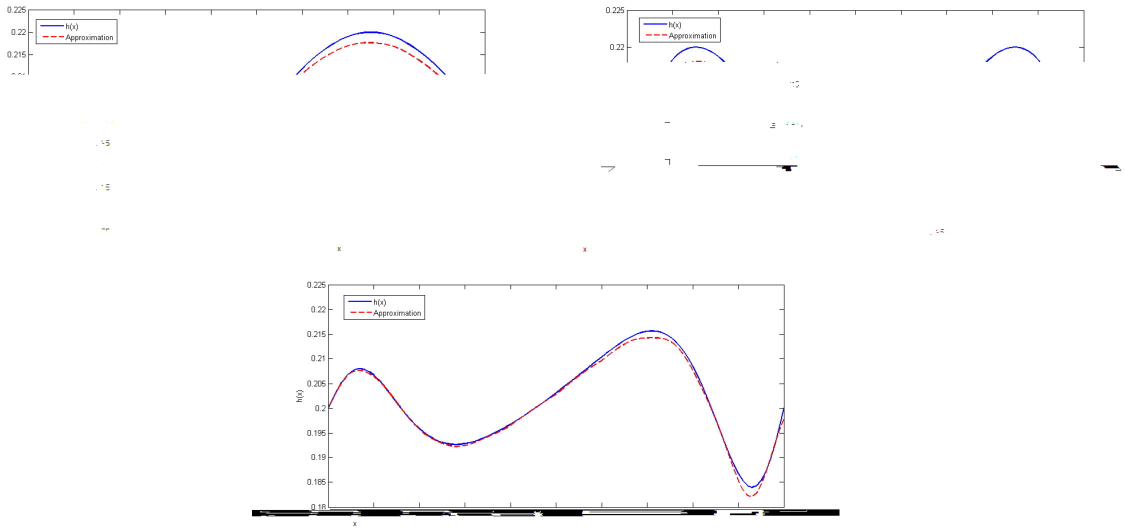

Figure A.7: Converged depth profiles for h_A, h_B and h_C respectively with $\nu_2 =$ Elp5iustislo(p)-27(2)]T6-3.319-4.4464Td[p(